EEE/CSC & ESAS SUPERCONDUCTIVITY NEWS FORUM (global edition), No. 42, October 2017.
Invited presentation M2OrC-01 given at CEC-ICMC 2017, July 09-13, 2017, Madison, WI (USA).

CEC/ICMC 2017 JULY 9-13 MONONA TERRACE MADISON, WI
M2OrC
2017 Cryogenic Engineering Conference and International Cryogenic Materials Conference
July 9-13, 2017, Madison, Wisconsin, USA

Development of Superconducting PM Machines

Potential application of cryo-magnets thanks to magnetization of RE-123 bulk superconductors

Mitsuru IZUMI[1] and Mark Ainslie[2]

[1]Tokyo University of Marine Science and Technology
[2]University of Cambridge

National University Corporation TUMSAT Tokyo University of Marine Science And Techology
WORLD'S BEST SMALL UNIVERSITIES 2016 tinyversity
UNIVERSITY OF CAMBRIDGE

Scope 1. High Temperature Bulk Superconductors

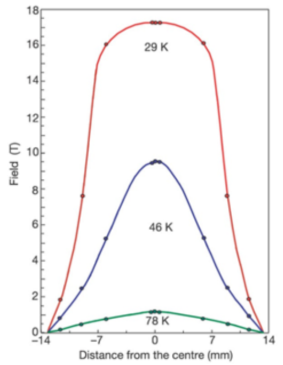

Trapped Field 17.24 T at 29 K
Masaru Tomita and Masato Murakami
Nature **421**, 517-520
-2003-

17.24 T could be trapped in a bulk Y-Ba-Cu-O sample of 2.65 cm diameter at 29 K

New/Guinness Record Trapped Field 17.6 T
in a stack of two, silver-doped Gd-Ba-Cu-O bulks
J.H. Durrell *et al*., Supercond. Sci. Technol. 27 082001
Cambridge group
-2014-

Large-grain (RE)$Ba_2Cu_3O_{7-\delta}$ ((RE)BCO) bulk superconductors exhibit large trap magnetic fields and have been studied with their critical current and reinforcement to protect against large Lorentz force.

A trapped field of 17.6 T has been reported from Cambridge group in a stack of two silver-doped GdBCO superconducting bulk samples, each 25 mm in diameter, fabricated by top-seeded melt growth and reinforced with shrink-fit stainless steel.

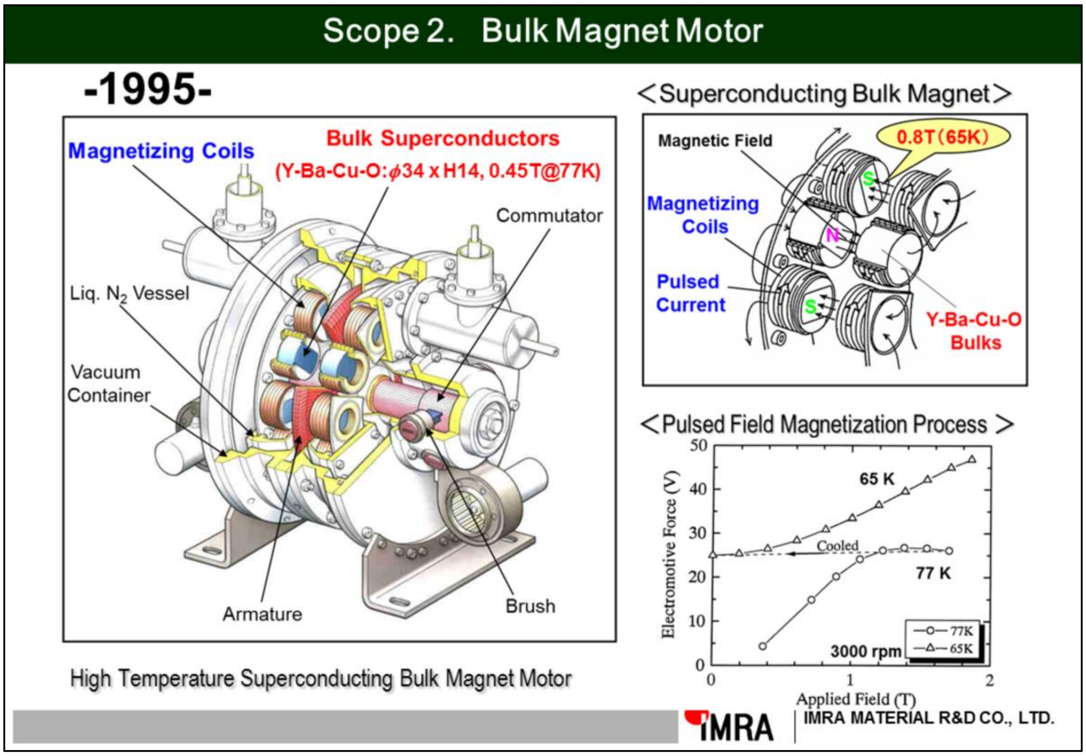

<Construction of the motor>

Twenty YBCO bulks 34 mm in diameter and 14 mm in thickness are mounted as field magnets in a disk-type print motor. Trapped fields of the twenty bulks magnetized by FC mode at 77 K ranged from 0.41 to 0.52 T, and the mean value was 0.45 T. Magnetizing coils are wound around the YBCO bulks in series so that their winding directions alternate. Ten YBCO bulks with the magnetizing coils are sealed in a liq. N2 vessel. Two sets of vessels containing the YBCO bulks are placed 18.8 mm apart from each other face to face, and a disk-shaped armature is placed between them. An armature current is commutated so as to flow radially in the same direction between each pair of facing YBCO bulks but in the opposite direction between neighboring pairs. Liquid nitrogen is filled in a pair of vessels. After cooling to below Tc (= 92 K), the YBCO bulks are simultaneously magnetized by feeding a pulsed current with a rising time of 2.4 ms to the magnetizing coils.

<Magnetization behavior>

Magnetization property of the set of twenty YBCO bulks was evaluated by measuring the electromotive force at 3000 rpm when the applied pulsed field is increased stepwise from 0.16 to 1.7 T at 77 K and subsequently from 0 to 1.86 T at 65 K. The temperature of 65 K was achieved by evacuating the vessels filled with the liquid nitrogen. In this magnetization process, the trapped field of the YBCO bulks at 65 K was increased by 1.8 times as high as at 77 K. The magnetic field between the facing YBCO bulks was 0.8 T.

<Reference>

・Jpn. J. Appl. Phys. Vol. 34 (1995) 5574-5578.

The HTS bulk magnet motor was mounted on a golf cart and was driven by a DC 36 V battery. The YBCO bulks were cooled to 65 K by evacuating the vessels filled with the liquid nitrogen, and were magnetized by feeding a pulsed current several times to the magnetizing coils. When stepping on the accelerator pedal, the HTS bulk motor car smoothly moved off.

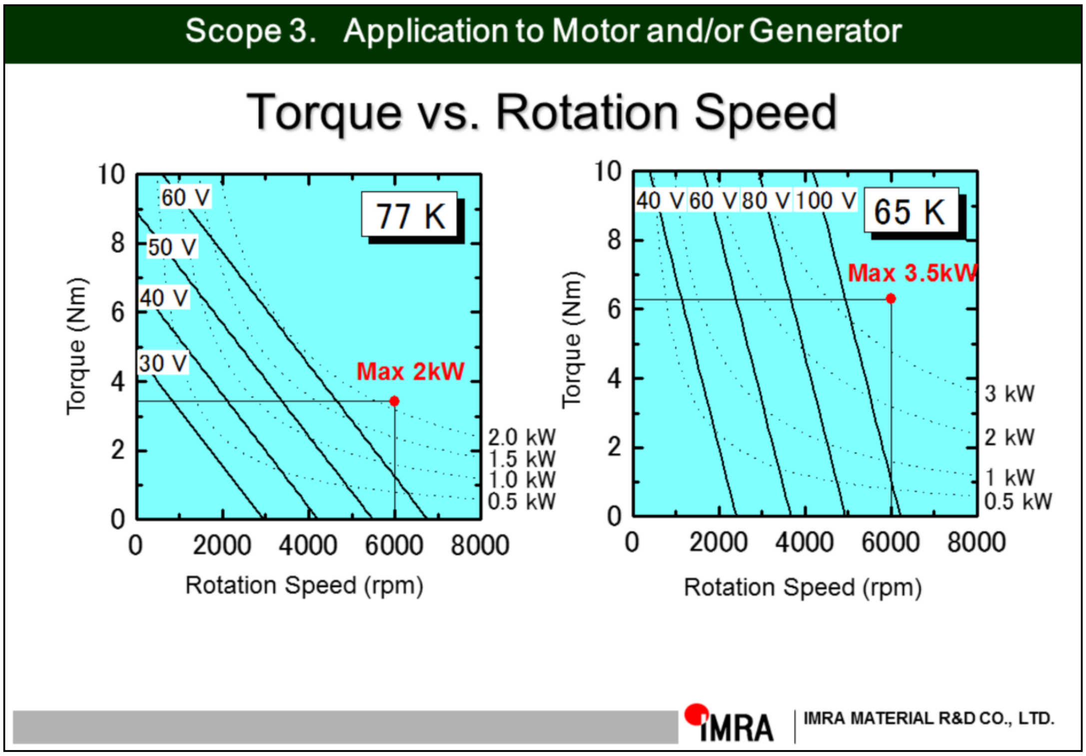

Output power of the HTS bulk magnet motor was limited by the maximum rotation speed of 6000 rpm and the maximum armature current of 40 A. The maximum output power was 2 kW at 77 K and 3.5 kW at 65 K.

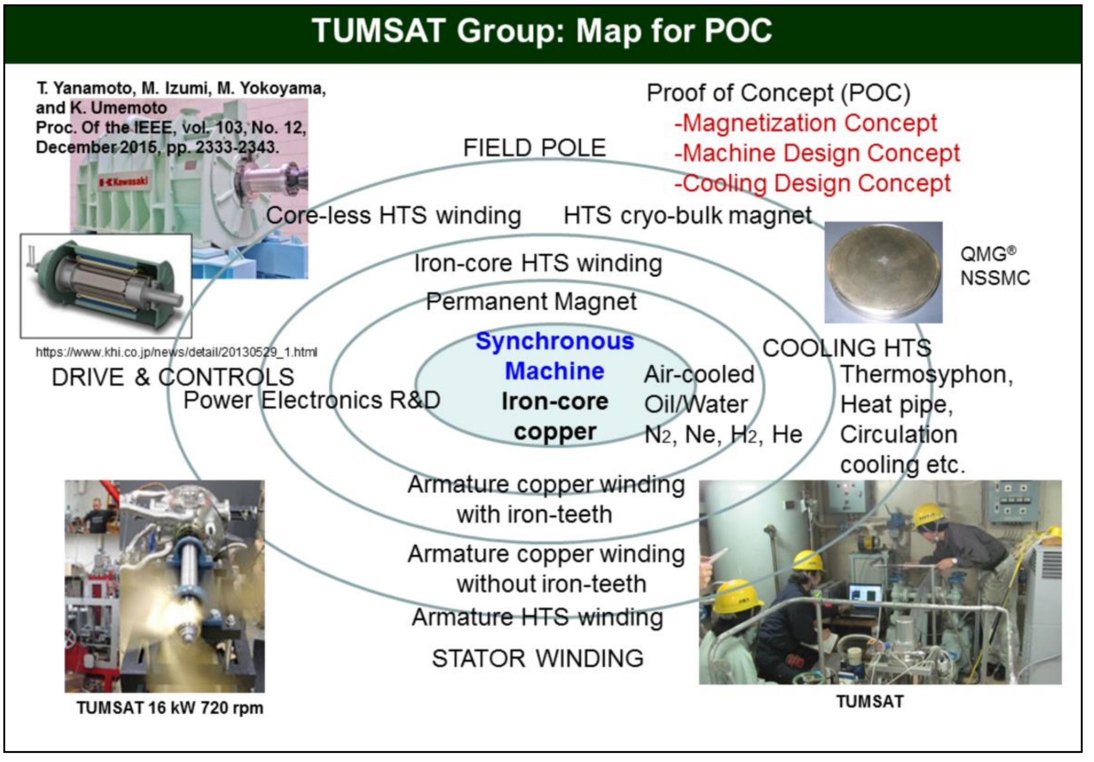

Since 2002, the research group of Tokyo University of Marine Science and Technology (TUMSAT) initiated the research and development of the marine propulsion motor/generator which used the HTS material as a field system.

This slide shows our R&D road/POC map together with the outcome test machine under industry-academia collaborations.

1. Magnetization Concept

Pulsed Field Magnetization

U. Mizutani and H. Ikuta (2000-2001 IMRA)
A. B. Surzhenko et al., M. Sander et al.
H. Fujishiro, IWATE Univ. (MMPSC)
T. Ida et al., TUMSAT Phsyica C 412-414, 638-645 (2004).
E. Morita et al., TUMSAT (CMDC)
Supercond. Sci. Technol. 19(12) , 1259-1263 (2006).
M. Tsuchimoto and K. Morikawa (Disks)
H. Ohsaki et al. (Rings)
S. Braeck, T.H. Johansen et al. (2002)
"Bulk HTS subjects to AC fields"
P. Vanderbemden et al.
(SUPRATECS/U of Cambridge)

PFM using waveform control (WCPM)
T. Ida et al. J. of Phys: Conf. Ser., 695, no. 1 12009 (2016).

T. Ida *et al.* (2004)

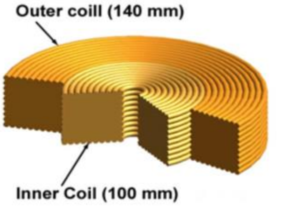

E. Morita *et al.* (2006)

The pulsed magnetization (PFM) is a promising technology necessary to practically use HTS bulk as a high-performance magnet.

During the PFM, local heat generation due to the flux motion which increase within the bulk in a short time.

TUMSAT group has developed a technique to magnetize HTS bulk in a motor. The PFM magnetizes the HTS bulk by using armature copper coils those should be inside the electric machines.

They have introduced a split vortex type coils which play a role of armature windings in case of axial-flux type rotating machines.

TUMSAT group also attempted to magnetize the field pole bulks efficiently with a CMDC (Controlled Magnetic density Distribution Coil) composed of the outer solenoid and the inner vortex.

In general, the pulsed field is not suitable for magnetizing to HTS bulk because a transient response of the LCR circuit generates magnetic field.

However, WCPM of TUMSAT, which is shown in the following slides, enables pulse magnetization by the magnetic field waveform optimized for magnetic field capture of the HTS bulk.

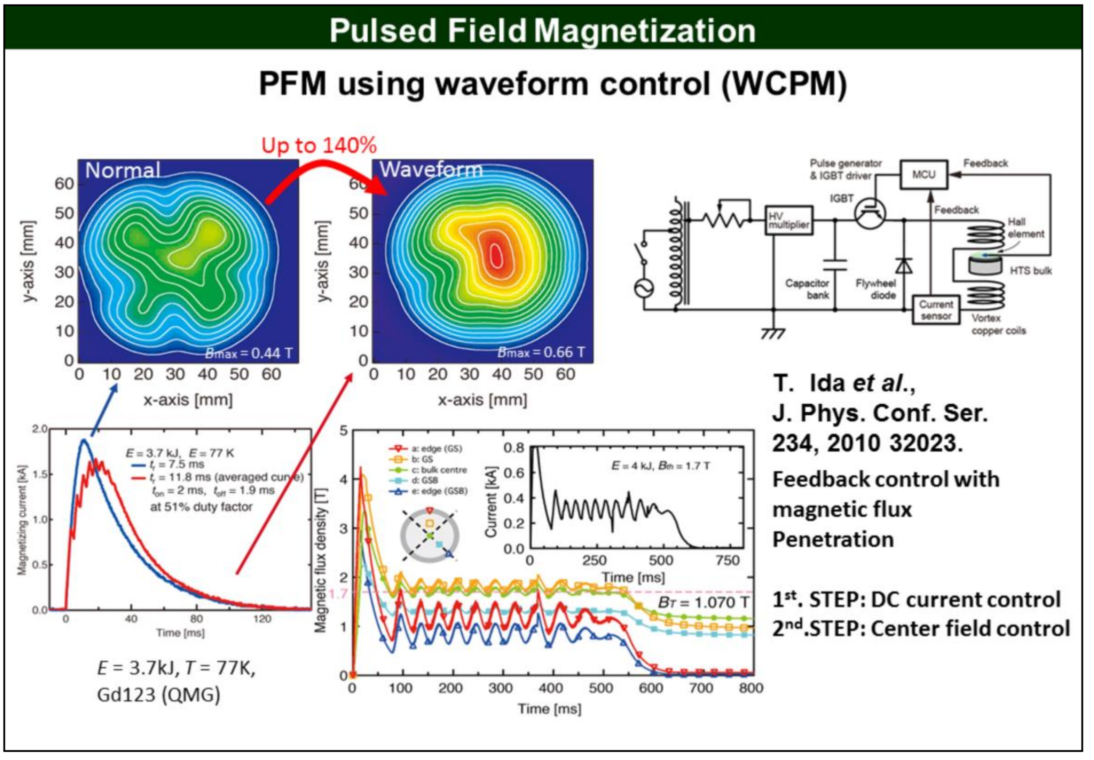

The PFM which LCR circuit generated gave the trapped distorted magnetic field distribution, low magnetic flux density and total magnetic flux to the HTS bulk.

However, trapped magnetic flux density and total magnetic flux increased by 140% and obtained conical magnetic field distribution when they applied pulsed magnetic field of the same energy and slightly different waveform to HTS bulk.

This result shows that waveform of the pulsed field has a influence on trapped magnetic field characteristic of the HTS bulk.

Thus trapped magnetic field may greatly improve by forming the pulse magnetic field from the penetration magnetic flux into the HTS bulk, or the magnitude of the pulse current.

Pulsed Field Magnetization

Waveform Control Pulsed Field Magnetization (WCPM)

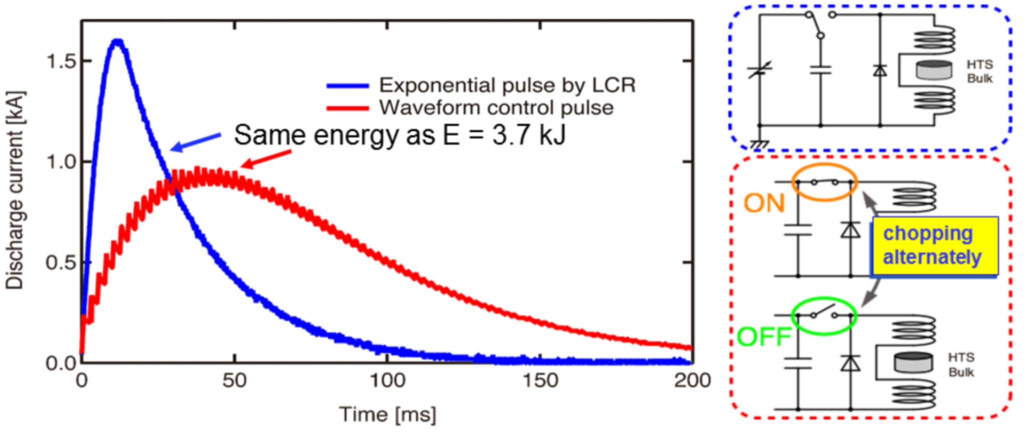

T. Ida, K. Shigeuchi, S. Okuda, M. Watasaki, M. Izumi, J. of Phys: Conf. Ser., 695, no. 1 12009 (2016).

The pulsed magnetic field generated from LCR circuit shapes waveform according to an exponential function.

WCPM forms the pulsed magnetic field waveform by chopping the current from the LCR circuit.

By the way, the vibration included in the waveform of the pulsed magnetic field does not adversely affect trapped magnetic field characteristics.

Pulsed Field Magnetization

WCPM by magnetic flux density feedback

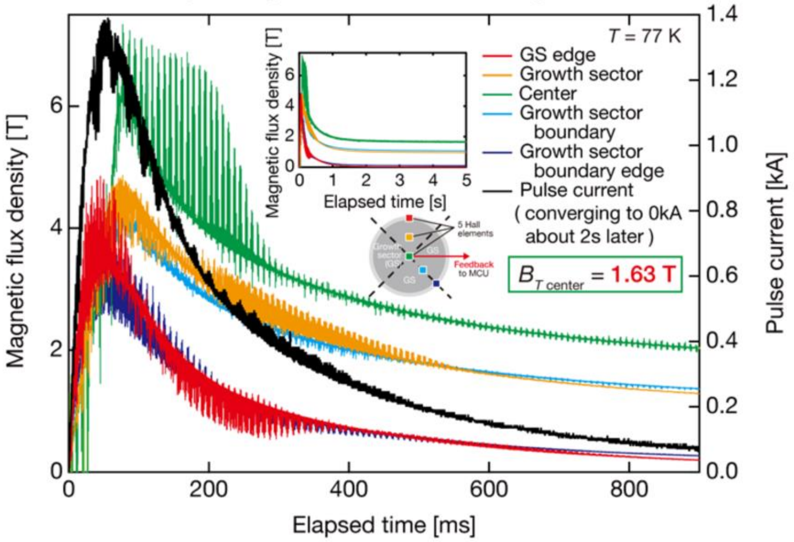

T. Ida, K. Shigeuchi, S. Okuda, M. Watasaki, M. Izumi, J. of Phys: Conf. Ser., 695, no. 1 12009 (2016).

A QMG (NSSMC) with a diameter of 45 mm and a thickness of 19 mm, which trapped 1.7 T by FC at 77 K, was magnetized by the WCPM method.

After pulse magnetization at 77 K for 2 seconds only once, this HTS bulk trapped a magnetic field with a high magnetic flux density of 1.63 T in a conical shape.

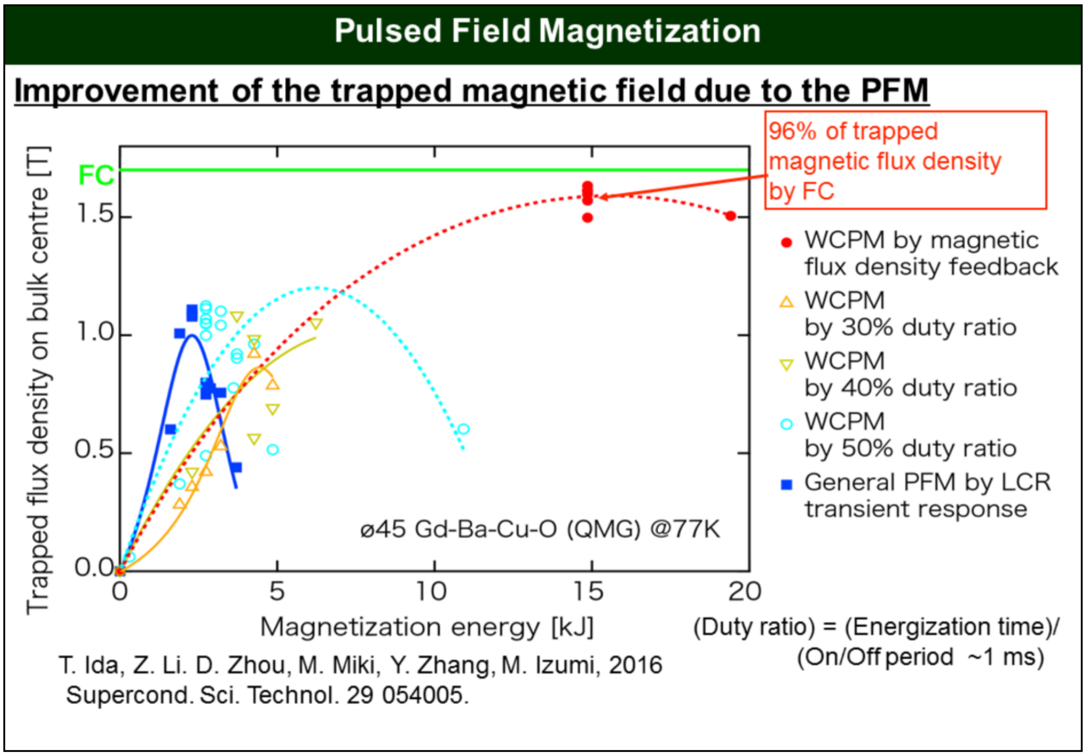

The trapped magnetic field characteristic of the HTS bulk deteriorates by pulsed field of the large energy.

Therefore the pulsed field generated by the LCR circuit got the considerably lower trapped magnetic flux density and total magnetic flux than FC.

By the WCPM method, the HTS bulk obtain energy greater than the LCR transient response pulsed magnetic field.

When the pulse magnetic field was shaped by the feedback information of the magnetic flux into the HTS bulk, HTS bulk obtained 6 times large energy of the LCR-PFM, and achieved 96% of the maximum trapped magnetic flux density of FC.

2. Machine Design Concept

Motor/Generator Design and POC

10 kW 720 rpm

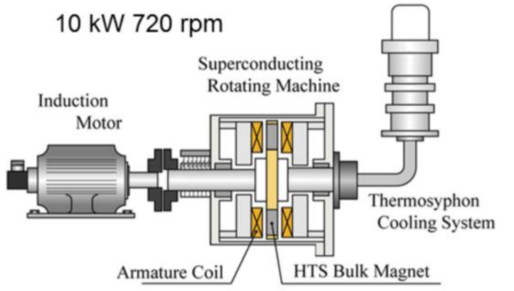

Fig. 1. Schematic drawing of the experiments. Induction motor as a prime mover was connected to the HTS bulk generator. The field pole bulks on the rotor are cooled down to 40 K with a closed-cycle thermosyphon with neon gas. The armature copper windings are cooled down by a flow of liquid nitrogen. The armature windings are composed of six pairs of the split-type coils as U, U′, V, V′ and W, W′ with 12 concentration winding copper coils. Eight field pole HTS bulks are on the rotor [2]–[4]. The armature coils and field poles are cooled down by liquid neon and liquid nitrogen.

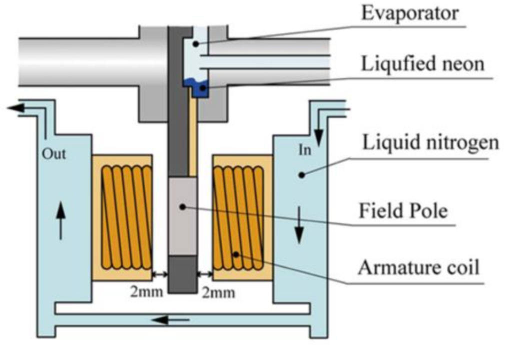

Fig. 2. Schematic drawing of the structure of superconducting rotating machine. The field poles were cooled down to 40 K by thermal conduction from evaporator. Liquid nitrogen was used for cooling down the armature coils. During rotation, the field pole was passed through upon 2 mm from the surface of armature coils.

M. Watasaki, M. Miki, B. Felder, K. Tsuzuki, R. Sato, S. Kase, M. Izumi, T. Ida,
IEEE Trans Appl. Supercond. **23** 6397585 (2013).

In our laboratory of TUMSAT, we have developed an axial gap type synchronous rotating machine with eight HTS bulk magnetized as the field poles [2], [3]. The bulk HTS magnets are magnetized by a couple of vortex type copper armature coils with pulsed current excitation [1]–[5].

[1] M. Tomita and M. Murakami, “High-temperature superconductor bulk magnets that can trap magnetic fields of over 17 tesla a 29 K,” Nature, vol. 421, pp. 517–520, Jan. 30, 2003.

[2] H. Matsuzaki, Y. Kimura, I. Ohtani, M. Izumi, T. Ida, Y. Akita, H. Sugimoto, H. Miki, and M. Kitano, “An axial gap-type HTS bulk synchronous motor excited by pulsed-field magnetization with vortex-type armature copper windings,” IEEE Trans. Appl. Supercond., vol. 15, pp. 2222–2225, 2005.

[3] H. Matsuzaki, Y. Kimura, I. Ohtani, E. Morita, H. Ogata, M. Izumi, T. Ida, H. Sugimoto, M. Miki, and M. Kitano, “Mechanical design of a synchronous rotating machines with Gd-Ba-Cu-O HTS bulk pole-field magnets operated by a pulsed-field magnetization with armature copper coils,” J. Phys., vol. 43, pp. 776–779, 2006.

[4] T. Sano, Y. Kimura, D. Sugyo, K. Yamaguchi, M. Izumi, T. Ida, H. Sugimoto, and M. Miki, “Pulsed-field magnetization study for Gd123 bulk HTS cooled with condensed neon for axial-gap type synchronous motor,” J. Phys., vol. 97, pp. 12 194–12 201, 2008.

[5] H. Mats zaki, Y. Kimura, E. Morita, H. Ogata, T. Ida, M. Izumi, H. Sugimoto, M. Miki, and M. Kitano, “HTS bulk pole-field magnets motor with a multiple rotor cooled by liquid nitrogen,” IEEE Trans. Appl. Supercond., vol. 17, pp. 1553–1556, Jun. 2007.

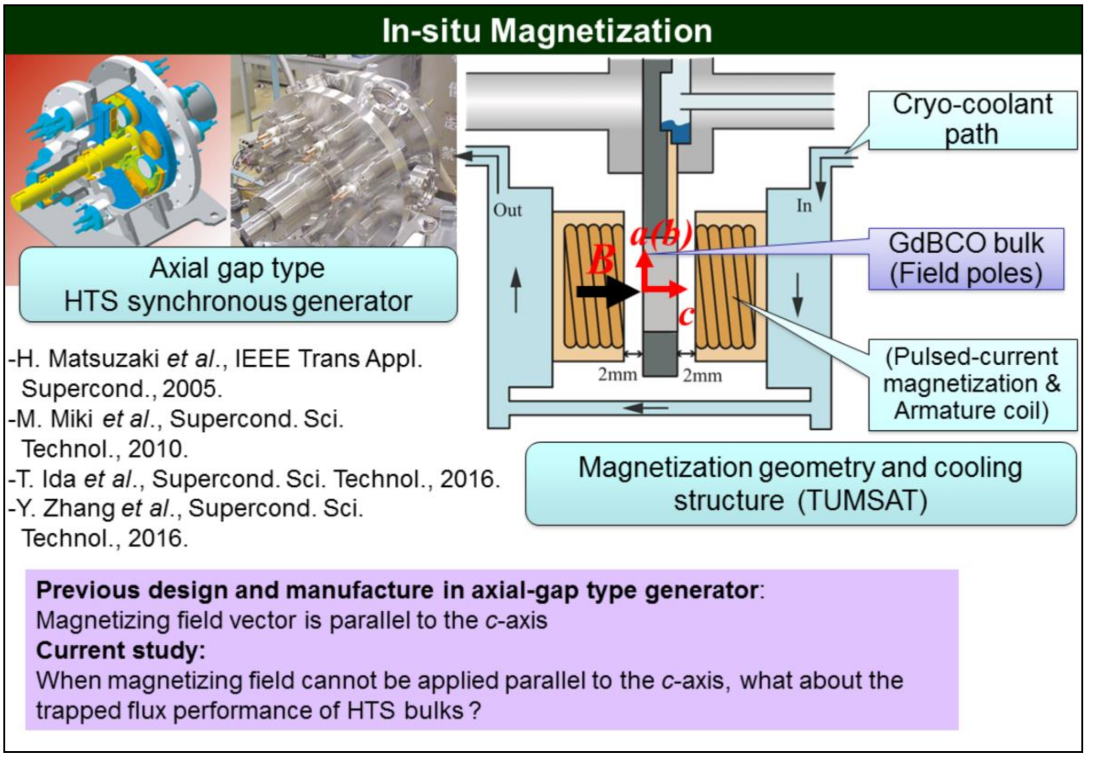

A single grain bulk high-temperature superconductor (HTS) exhibits intensified flux trapping performance upon field cooled magnetization. The world record of trapped flux is 17.6 T

achieved by using stacked two-fold GdBCO bulks. However, the majority of magnetization studies focused on the magnetization along the crystallographic c-axis. In the present study, we

clarify the flux trapping performance under field cooled magnetization using an off-axis magnetic field with respect to the *c*-axis.

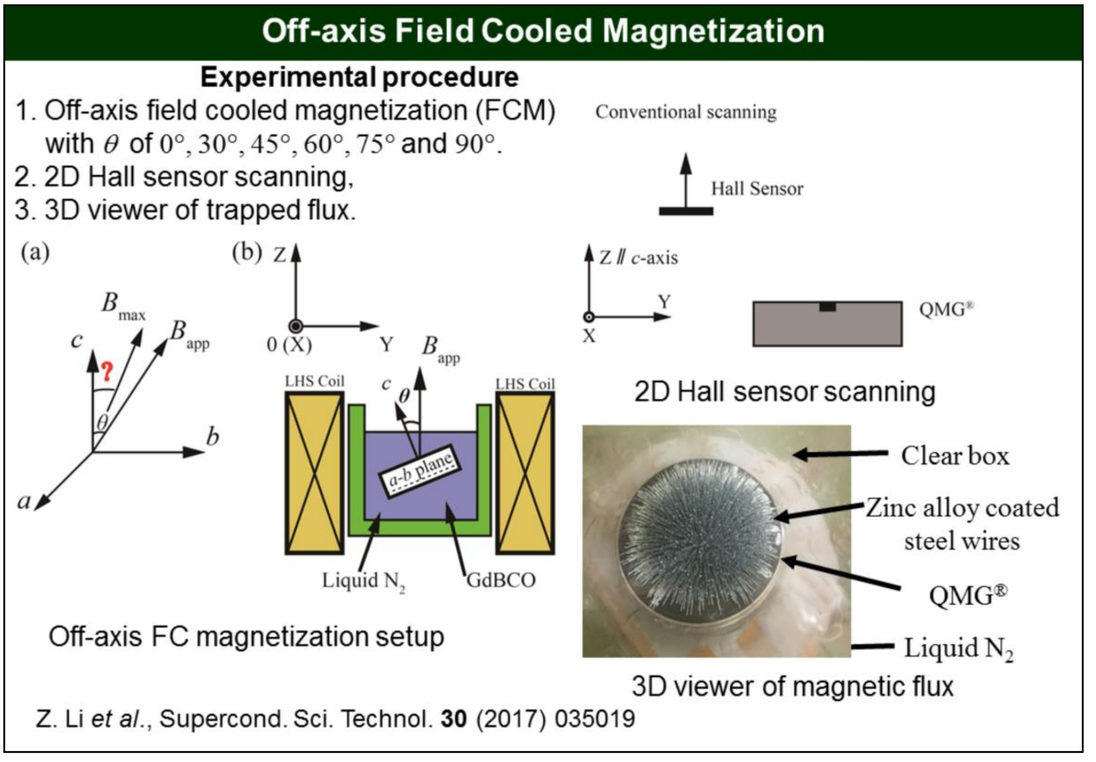

A GdBCO-QMG® sample of 60 mm in diameter and 20 mm in thickness prepared by Nippon Steel & Sumitomo Metal Corporation was employed to investigate the trapped flux behaviour using off-axis FCM as shown.

To apply the magnetizing field, we have employed a 5 T superconducting magnet by Japan Magnet Technology. The field sweep rate was set at 1.39 mT s−1 during the magnetization processes. The bulk was mounted on a self-designed sample holder to keep the angle θ with respect to the c-axis of the bulk at 30° , 45° , 60° , 75° and 90° and was cooled down by immersing into a liquid N2 bath under 3 T (Bapp) gradually.

Once temperature stability was achieved, the applied field was removed. After the removal of the external field, the trapped flux measurement, using a Hall sensor (F W BELL, model BHT-921), was started after 75 min to eliminate the major flux creep.

Off-axis Field Cooled Magnetization

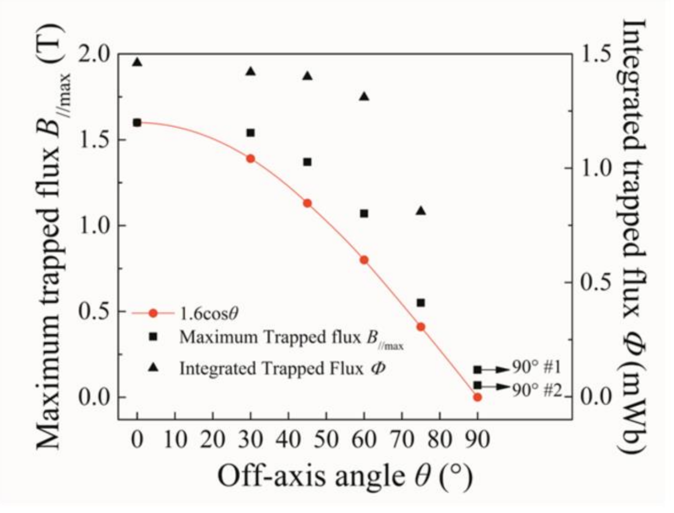

Angular dependence of trapped flux under on and off axis FCM with θ of 0°, 30°, 45°, 60°, 75° and 90°. 90° #1 and 90° #2 represent the trapped flux under FCM with aligned growth sector boundary and misaligned growth sector boundary geometry when θ is 90°, respectively.

Z. Li *et al.*, Supercond. Sci. Technol. **30** (2017) 035019.

The results show that the trapped flux is almost polarized along the applied field as expected. This tendency remains up to a high off-axis angle θ around 60° . It is worth mentioning that, with θ of 30° , the maximum trapped flux component B//max parallel to the c-axis significantly remains more than 96 % of 1.6 T which occurs under on axis magnetization. Meanwhile, the angular dependence of the c-axis parallel component exhibits that observed flux density is higher than that expected from 1.6 cosθ. It is highly emphasized that the off-axis magnetization with the finite inclination angle is quite useful for introducing into the design of HTS applications.

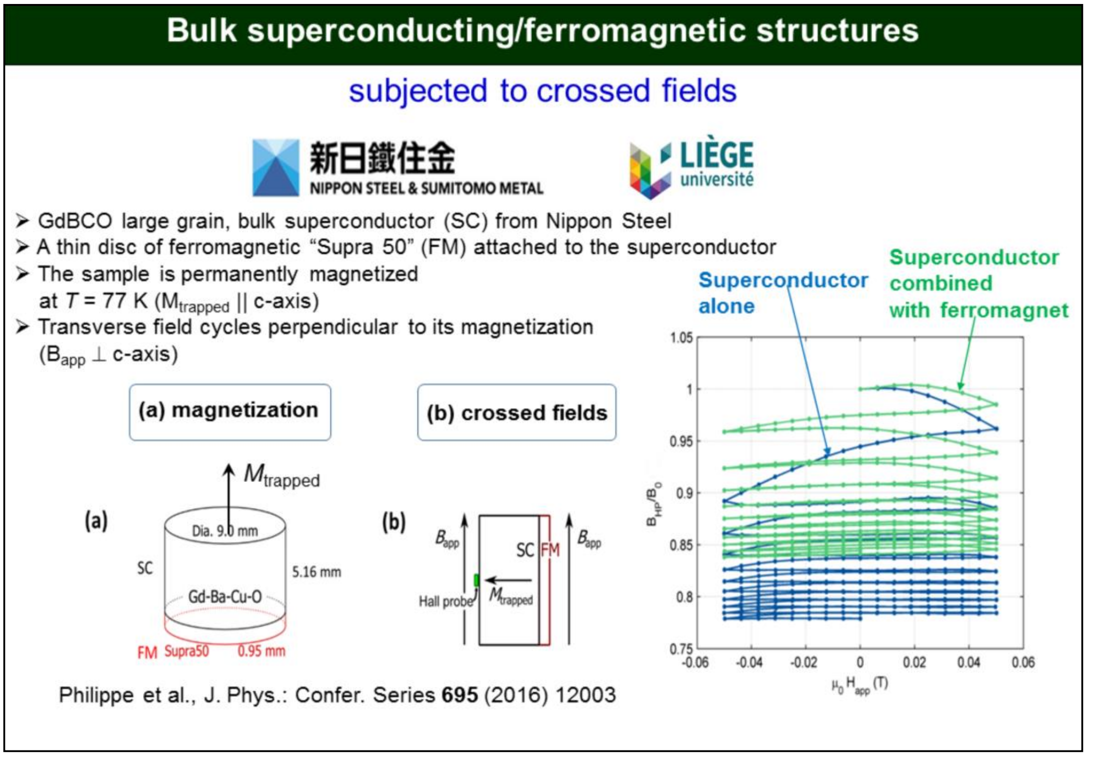

For a successful operation of the rotating machine, it is important to investigate the interaction of the bulk superconductor with the magnetic fields required for the operation of the device. This point was studied by the team from the University of Liege (Belgium), with recent investigations on bulk (RE)BCO samples provided from Nippon steel & Sumitomo metal (Japan). When the superconductor is placed in the rotor of a synchronous motor and subjected to the rotating field generated by the stator, transients that can arise e.g. during a sudden change of mechanical load in the device may lead to parasitic time-varying fields. These parasitic fields may substantially reduce the trapped flux density in the superconductor when their direction is orthogonal to that of the main magnetization, i.e. lead to "crossed-field demagnetization". In the work summarized in this slide, the team from Liege investigated the effect of a ferromagnetic disc placed against a bulk $GdBa_2Cu_3O_7$ superconductor from Nippon Steel when it is first fully magnetized (a) and then subjected to various cycles of transverse field (b) perpendicular to the trapped magnetic moment. The graph on the right shows the flux density measured by the Hall probe against the sample surface during 10 cycles of the crossed field (amplitude = 50 mT) for the superconductor alone (blue) and for the hybrid structure, i.e. the superconductor combined with the ferromagnet (green). Remarkably, the hybrid structure is much less affected by the transverse field than the superconductor alone. Such results give evidence that the addition of a ferromagnetic disc on one side of the superconductor reduces the collapse of the trapped flux density against the other face of the superconductor, which is important for rotating machine applications.

Bulk superconducting/ferromagnetic structures

subjected to crossed fields

新日鐵住金 NIPPON STEEL & SUMITOMO METAL

LIÈGE université

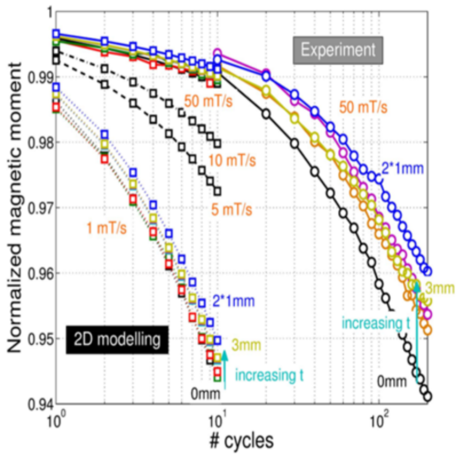

Comparison of the decay of the magnetic moment for various ferromagnet thicknesses and sweep rates

Fagnard et al., Supercond. Sci. Technol. **29** (2016) 125004

What has been done also is a detailed study of the influence of the geometry of the ferromagnetic part on both trapped fields and crossed field effects. The magnetic properties of the hybrid superconducting/ferromagnetic structures were characterized by measuring the magnetic moment with a magnetometer designed for large samples. The results were interpreted by means of 2D and 3D finite element models. This was done for various ferromagnet thicknesses and sweep rates of the crossed field. This kind of results is helpful to understand this phenomenon and have an importance for the design of rotating machines combining ferromagnets and superconductors.

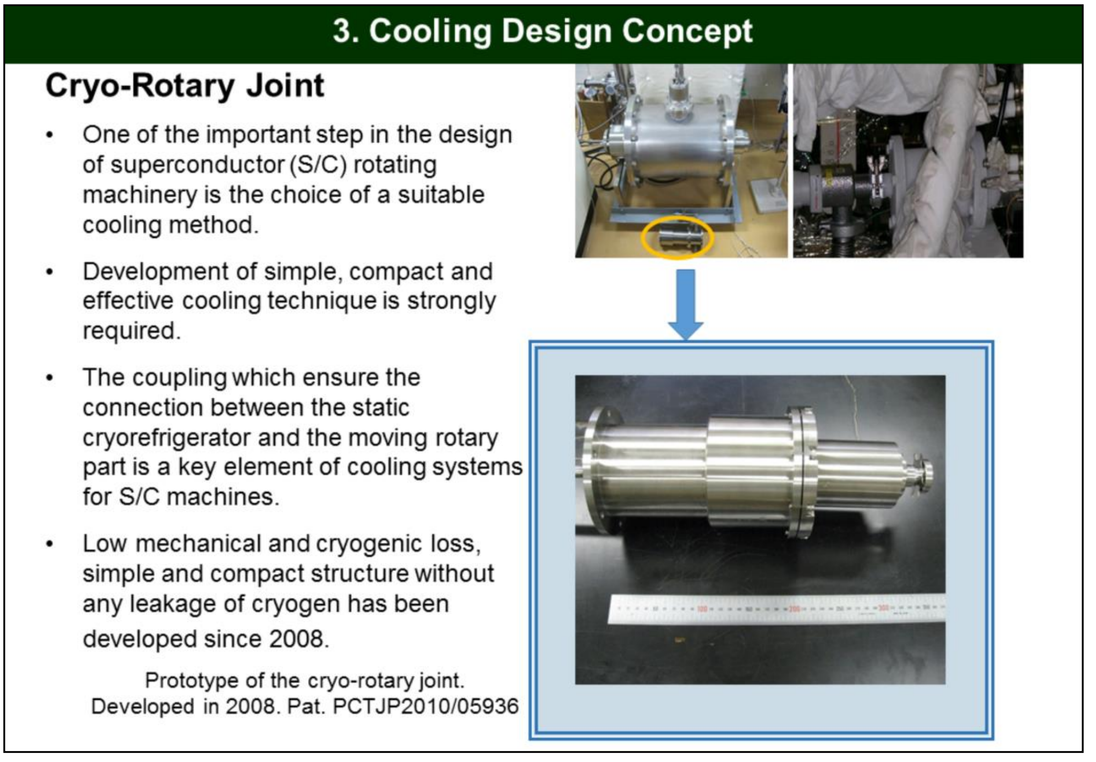

The cooling of high-temperature superconducting (HTS) rotating machinery is essential in many ways: enhancing the properties of the HTS material, ensuring safe and stable rotation, nullifying the effects of heat invasion from the outside or of a possible generation during operation, etc. It presents, however, a challenge, in the presence of the necessary cryogenic moving connection allowing the flow of cryogen into the rotor. Our laboratory has been developing cryogenic rotary joints applied to the flow of cryogenic condensed gases for many years, coupled to the thermosyphon technology at the liquid neon temperature. This paper deals with the evolution of the models through the years, to eventually emphasize the new-born model adapted to the 100-kW class marine propulsion HTS motors. The results were the absence of leak of the cryogen and a small heat invasion, even during a rotation test conducted at 90 rpm. The design of the cooling system of a 20-MW class propulsion motor is the final target.

[1] M. Miki, B. Felder, K. Tsuzuki, M. Izumi, and H. Hayakawa, “Development of the cryo-rotary joint for a HTS synchronous motor with Gd-bulk HTS field-pole magnets,” J. Phys., Conf. Ser., vol. 234, no. 3, 2010, Art. no. 032039

Cryo-Rotary joint

Key Features

Specifications of the cryo-rotary joint prototype

Overall length [mm / in]	348 / 13.7
Diameter [mm / in]	126 / 4.96
Weight [kg / lb]	12.6 / 27.8
Loss [W] @700rpm	6.36
Maximal rate [rpm]	1 000
Pressure range [MPa]	- 0.1 ~ + 0.45
Allowable heat transfer [W]	~ 100
Type of cryogen	Liquid and/or gaseous He, H_2, Ne, N_2, O_2, Ar

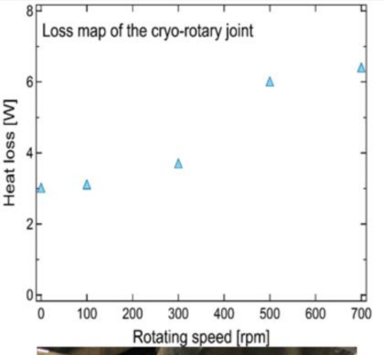

We have developed a new kind of cryogenic rotary joint aimed for 100-kW class high-torque ship propulsion HTS motors. The heat invading through the joint or being generated through rotation was less than 3 W, to be compared

with the overall available 100-W cooling power of the system. Concerning the sealing capacity of the joint, it proved its reliability on the rotating speed range of this kind of motors, from 0 rpm to 120 rpm. The vacuum level was only changed of a $1x10^{-5}$ Pa factor, negligible in motor applications. The design, directly attached on the shaft of the machine, makes it adaptable to bigger scales, like the targeted MW scale HTS motor

Thermosyphon cooling

- Helium gas forced circulation (20 -30 K) has been a typical technique to cool down S/C rotating machines.
- Closed cycle thermosyphon (TS) is another cooling system candidate, not only for rotating machines but also a variety of superconductor applications.
- TS features are simple and they benefit from compactness and the heat transfer rate.
- TUMSAT team has been studying the TS using neon and helium as a working fluid since 2006.

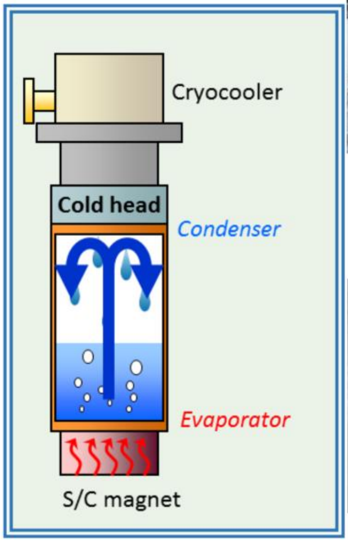

Fin array and condensation container in TUMSAT.

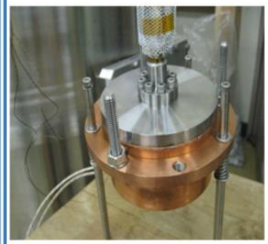

Evaporator in the center of rotor.

Temperature Superconductors (HTS) applied to rotating machines require an efficient cooling system. It is necessary to increase the maximum trapped flux density in the bulk HTS magnets and decrease the overall cooling time. In this paper, we added a gaseous helium phase to a condensed-neon closed-cycle thermosyphon. The latent heat of neon-film cooling is combined with helium's high thermal conductivity. Different mixture proportions were evaluated in terms of resistance to variable heat loads. More helium decreased the temperature variation of the evaporator. The mixture was then used to cool down a 30 kW-grade gadolinium-bulk HTS synchronous motor. The eight bulk HTS conductors of the rotor were cooled to 40 K in less than six hours. The application of this thermosyphon is envisioned for larger rotating machines.

[1] B. Felder, M. Miki, K. Tsuzuki, M. Izumi, and H. Hayakawa, “Optimization of a condensed–Neon cooling system for a HTS synchronous motor with Gd-bulk HTS field magnets,” J. Phys. Conf. Ser., vol. 234, 2010, Art. no. 032009.

Thermosyphon cooling

- The developed TS is firstly tested as stand-alone and then attached to prototype axial S/C motor for evaluation.
- Stable cooling, around 30 - 40 K, on the surface of the HTS bulk was confirmed even when the machine is rotating at 720 rpm.

Specifications of the Ne/He closed TS

Cooling power [W] @ 30 K	**85**
Power consumption [kW] @ 50 Hz	**6.7**
Working fluid	**Ne / Ne/He**

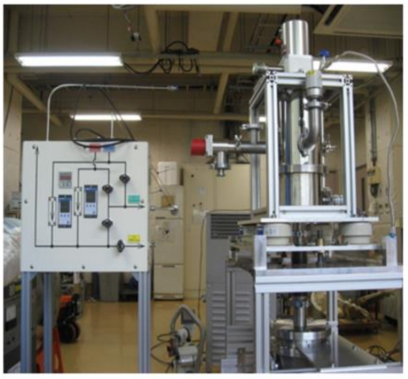

Developed closed cycle TS (Right) and gas flow control box (Left).

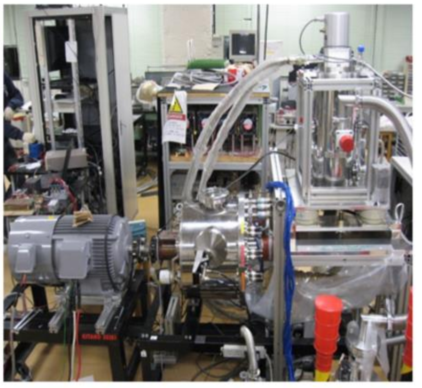

S/C motor coupled with Ne/He TS and cryo-rotary joint during load test.

Commercial high-temperature superconducting (HTS) wires restrain us to an operation temperature ranging from 20 to 40 K for field-pole magnets applied to rotating machinery. We have proposed to employ a mixture of helium and neon gas in a closed-cycle thermosyphon based on a GM cryo-refrigerator. In this paper, we discuss the temperature stability of the evaporator created by a helium-neon mixture cooling coupled with a closed-cycle thermosyphon, upon an external heat load on a 100-kW-grade HTS synchronous machine. A home-made cooling system, including the condenser, was designed. The evaporator was assembled within the motor in accordance with thermal and mechanical analysis. The cooling of the evaporator with the 100-kW-grade HTS synchronous motor was applied against a variable heat load equivalent with the actual HTS rotor field poles. We report these results and propose its potential application to a large-scale ship propulsion motor.

[1] B. Felder et al., “Development of a cryogenic helium-neon gas mixture cooling system for use in a Gd-bulk HTS synchronous motor,” IEEE Trans. Appl. Supercond., vol. 21, no. 3, pp. 2213–2216, Jun. 2011.

[2] B. Felder et al., “A 100-W grade closed-cycle thermosyphon cooling system used in HTS rotating machines,” in Proc. AIP Conf. Proc., 2012, vol. 1434, pp. 417–424.

[3] R. ato et al., “Helium-neon gas mixture thermosyphon cooling and stability for large scale HTS synchronous motors,” IEEE Trans. Appl. Supercond., vol. 23, no. 3, Jun. 2013, Art. no. 5200704.

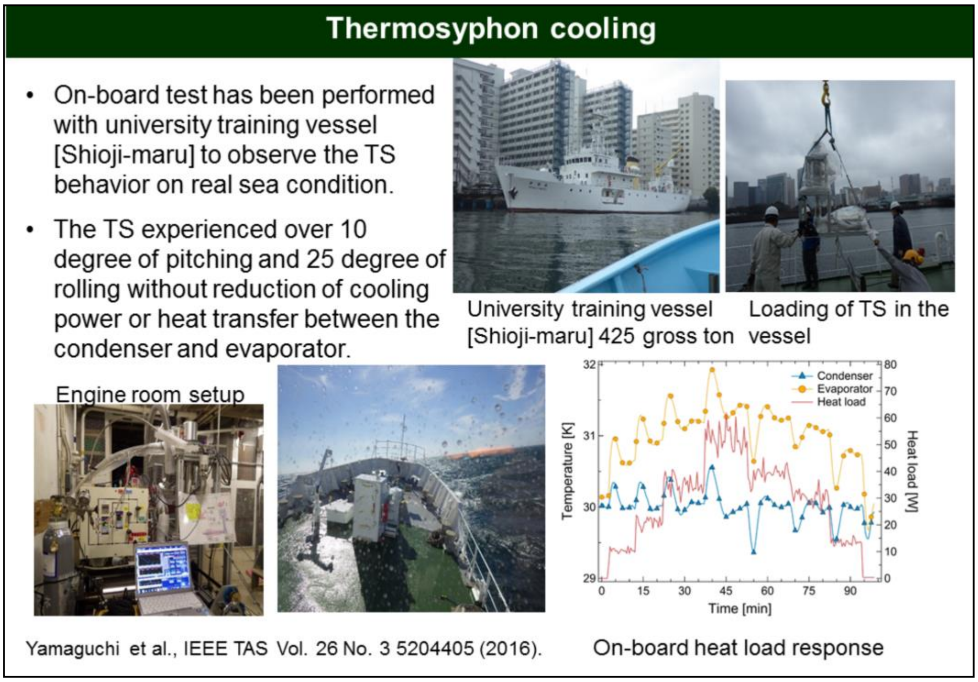

Thermosyphoning (TS) is a heat exchange mechanism that uses a circulating refrigerant based on natural convection with no need for a mechanical pump. This cooling technique has been employed to circulate liquid coolant and gaseous coolant for high-temperature superconductor (HTS) rotating machine systems. These machines operate with an HTS field pole in the temperature range from 25 to 40 K, which are suitable temperatures for the survivability of HTS wires. The cryomechanical components are simple; there are a condenser, an evaporator, and adiabatic tubes located between the condenser and the evaporator. For applications to ship propulsion motors or generators of the radial gap type, the liquid/gas coolant flow along the adiabatic tube inside the rotating shaft may be considerably affected by the ship's rolling and/or pitching motion. In this work, we studied the temperature stability and heat load survivability of cryogenic TS, by constructing a 100 W @ 30 K-grade model. We investigated the temperature, thermal resistance, and heat flux, with a maximum load up to 60 W, of ground and onboard tests. The observed TS behavior indicates that there is sufficient survivability to assemble megawatt-class ship propulsion systems.

High Power Density Superconducting Machines

1. Twinned rotor assembly for axial-type machines

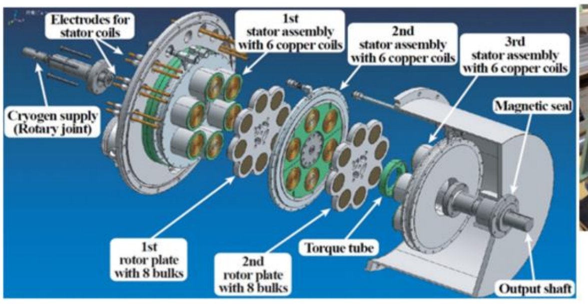

2. Miki et al., Novel Design of a 30 kVA Rotor System with Bulk High-Temperature Superconductor for a Motor/Generator, Abstract and presented in *Applied Superconductivity Conference*, ASC2014, Charlotte, NC, August 11, and M. Izumi and M. Miki, 2014 "Radial-gap type superconducting synchronous machine magnetizing apparatus, and magnetizing method," EP 3125415 A1, Feb. 2017, PCT/JP2015/059155.

TUMSAT

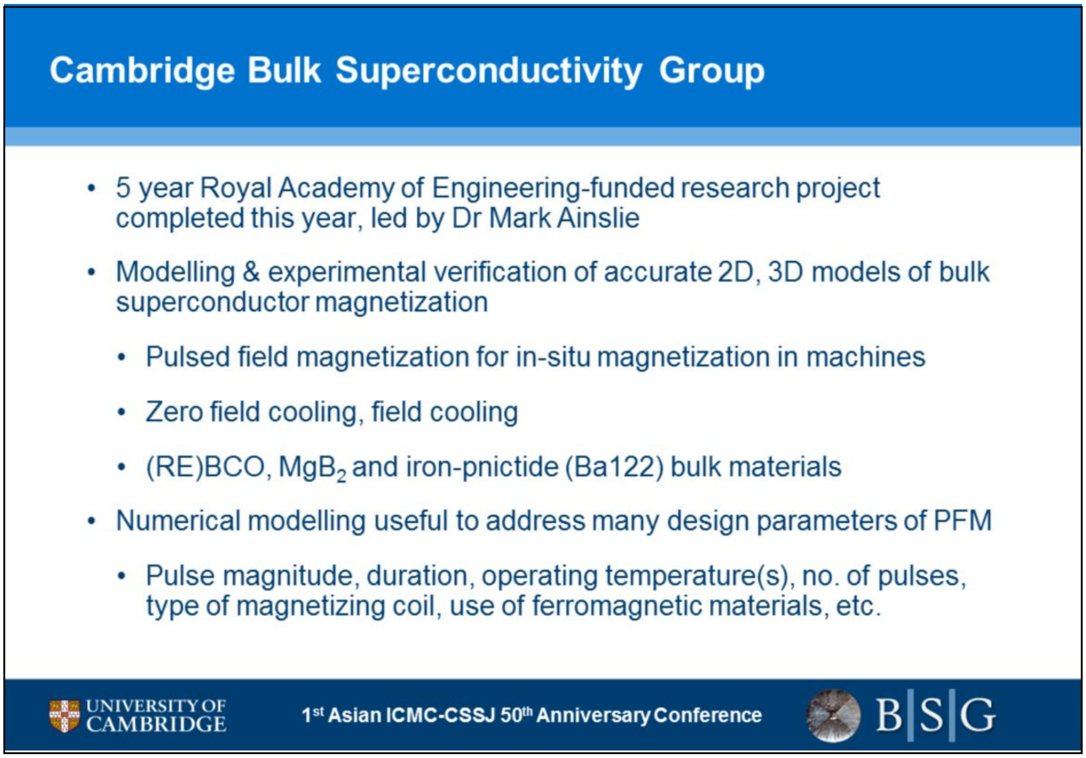

A team of researchers (led by Dr Mark Ainslie, Royal Academy of Engineering Research Fellow) in the Bulk Superconductivity Group, Department of Engineering, University of Cambridge has been investigating various aspects of superconducting machine design utilising both wire and bulk forms of high temperature superconducting (HTS) materials in a five-year project that was completed this year.

The research programme involved fundamental research to overcome some of the technical challenges associated with these superconductors, including investigating techniques to reduce AC loss in superconducting coils and investigating the magnetisation properties of bulk superconductors.

2D and 3D models of bulk superconductor magnetization have been developed to assess the performance of bulk superconductors under various conditions, including various pulsed field magnetization (PFM) analyses towards in-situ magnetization in machines, as well as zero field cooling and field cooling magnetization. The models can also predict the performance of different families of superconductors, including (RE)BCO, MgB_2 and iron-pnictide (Ba122) materials, systematically under different processing conditions.

Numerical modelling is particularly useful to address the many design parameters that exist for PFM, including the pulse magnitude and duration, operating temperature(s), number of pulses, the type of magnetizing coil(s), the use of ferromagnetic materials, and so on.

Split coil pulsed field magnetisation with an iron yoke

UNIVERSITY OF CAMBRIDGE

CEC/ICMC 2017

B|S|G

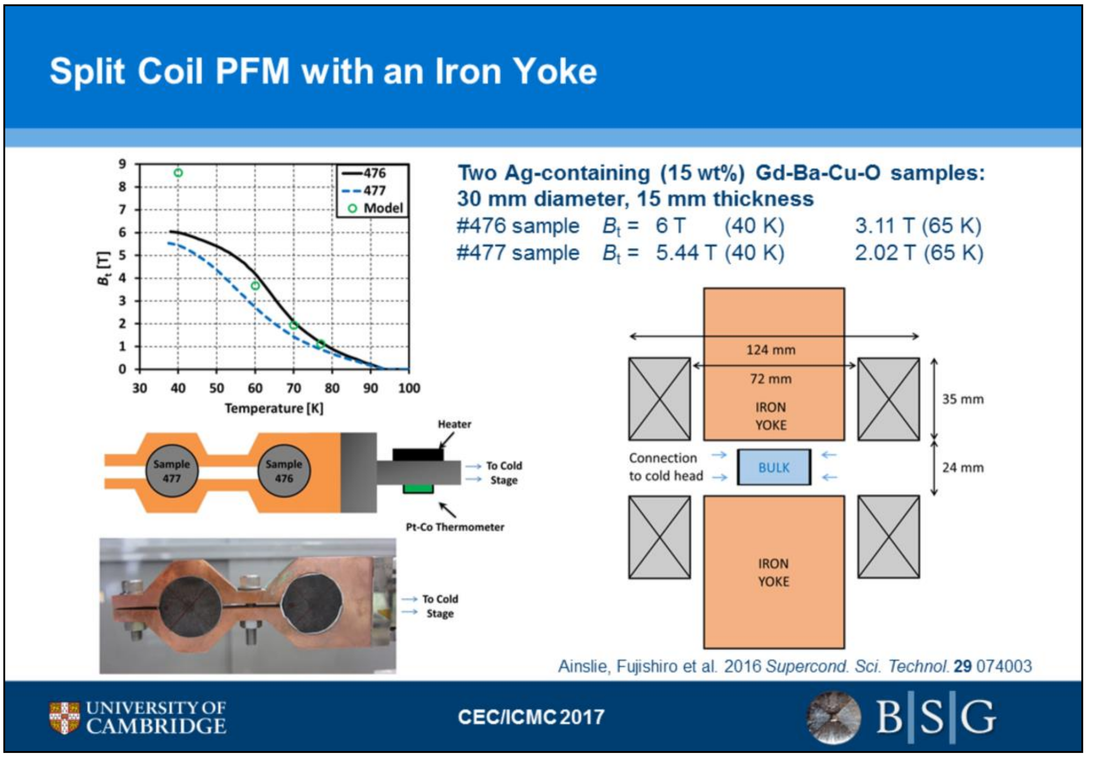

In this study, two Ag-containing (15wt%) Gd-Ba-Cu-O bulk superconductor samples were magnetized by PFM using a split coil with an iron yoke. The two samples (labelled #476, #477) were firstly field cooled from approximately 40 K in a 7 T background field, trapping 6 T and 5.44 T at 40 K and 3.11 T and 2.02 T at 65 K, respectively. These results, as well as the modelling results described later, are compared in the top left figure. Shown on the bottom left of the slide is the sample holder, made from copper, for the split coil PFM experiments. The sample holder is connected to the cold stage of a Gifford-McMahon cycle helium refrigerator in a vacuum chamber that has a small vacuum space of 1 mm.

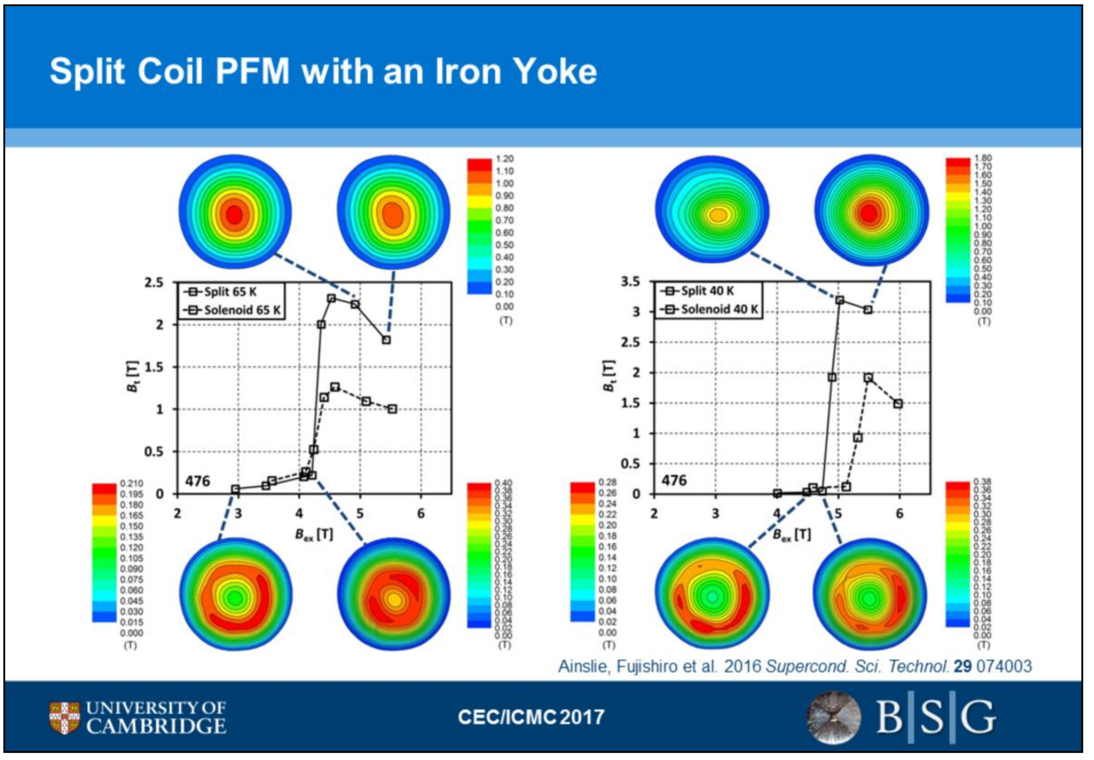

These figures show the 2D trapped field distributions at 65 K (left) and 40 K (right) for sample #476 after magnetization by PFM using the split coil with the iron yokes inserted, and these were measured on the outside surface of the vacuum chamber (approximately 2 mm above the bulk surface) by scanning a Hall sensor using an x-y stage controller. The trapped field at the centre of the top surface of the sample magnetized by PFM using the split coil (with the iron yokes inserted) and a solenoid coil (also with an iron yoke embedded in the cold stage, under the sample) are also compared in the inset figures, which clearly show that the split coil arrangement results in a larger measured field.

Numerical Modelling Example

2D axisymmetric model, Maxwell's equations

$$\nabla \times \mathbf{E} = -\frac{\partial \mathbf{B}}{\partial t} = -\frac{\partial(\mu_0\mu_r\mathbf{H})}{\partial t}$$ Faraday's Law

$$\nabla \times \mathbf{H} = \mathbf{J}$$ Ampere's Law

$$\mu_r = \mu_{r,\,max} \text{ for } B < \mu_0 M_{sat}$$

$$\mu_r = \left(1 + \frac{M_{sat}}{H}\right) \text{ for } B \geqslant \mu_0 M_{sat}$$ Ferromagnetic material

Magnetising fixture simulated using a copper coil sub-domain

Cooling simulated using a cold head + vacuum chamber

Effect of iron yoke in bore of split coil analysed for trapped field enhancement

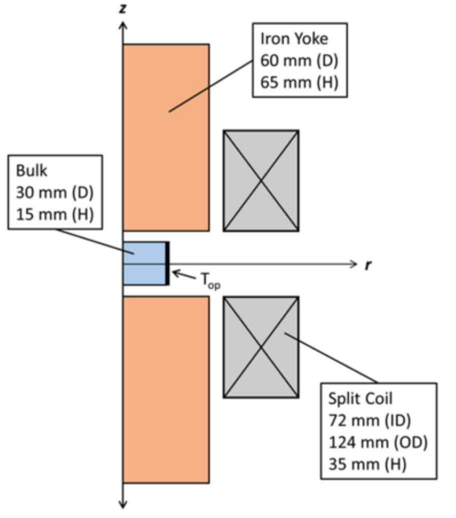

UNIVERSITY OF CAMBRIDGE CEC/ICMC 2017 B|S|G

In order to explain how this works, numerical simulations using a 2D axisymmetric finite element method based on the ***H***-formulation (for which the governing equations are derived from Maxwell's equations) were carried out to qualitatively reproduce and analyse the magnetization process from both electromagnetic and thermal points of view. The magnetizing fixture is simulated using a copper coil sub-domain and cooling is simulated by a cold head (fixed temperature boundary) within a vacuum chamber. Measured and literature values were used for the thermal properties of the materials included. The effect of the iron yoke in the bore of the split coil is analysed and the relative permeability of the iron is approximated using a linear permeability $\mu_{r,max}$ = 2000 and a saturation field $\mu_0 M_{sat}$ = 1.6 T.

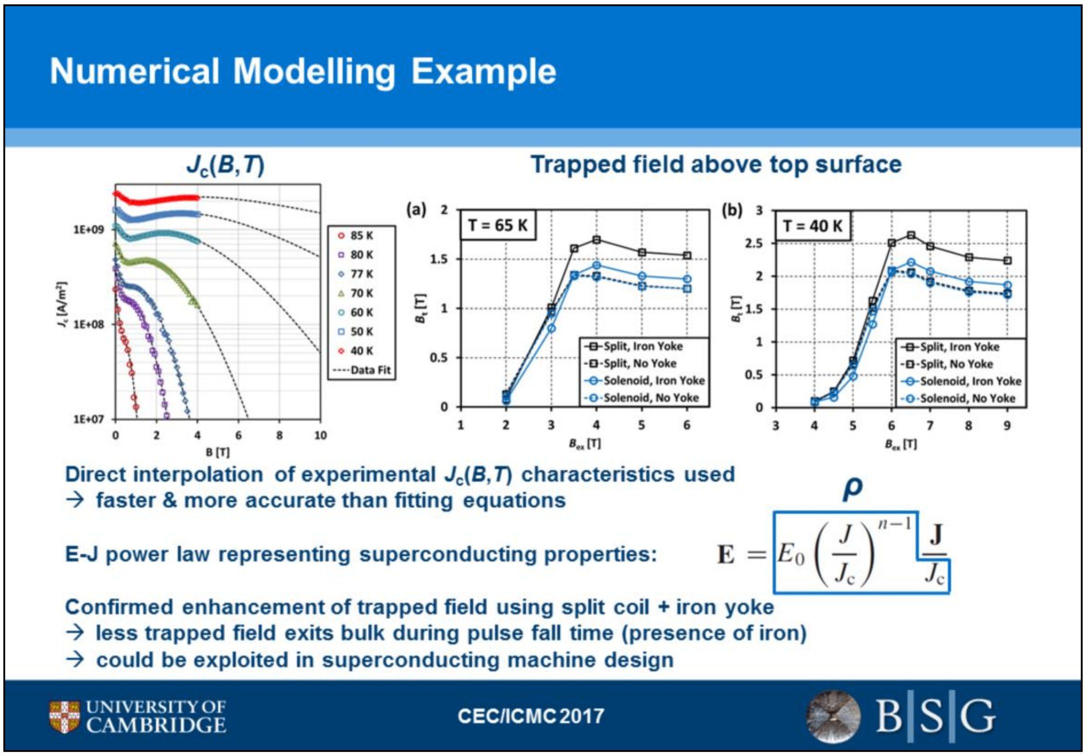

A direct interpolation of the experimentally measured $J_c(B,T)$ characteristics (see top left figure) of a small, representative sample was used to increase the computational speed of the models, which is both faster and more accurate than using fitting equations. The *E-J* power law is used to represent the superconductor's electrical properties.

The model confirmed the enhancement of the trapped field using the split coil with the iron yoke, and it is shown that after the pulse peak, less flux exits the bulk when the iron yoke is present, resulting in a higher peak trapped field, as well as more overall trapped flux, during the pulse fall time. Such a split coil arrangement could be exploited in an axial gap-type superconducting electric machine to improve the trapped field and increase the effective air-gap magnetic field.

Flux jump-assisted pulsed field magnetisation

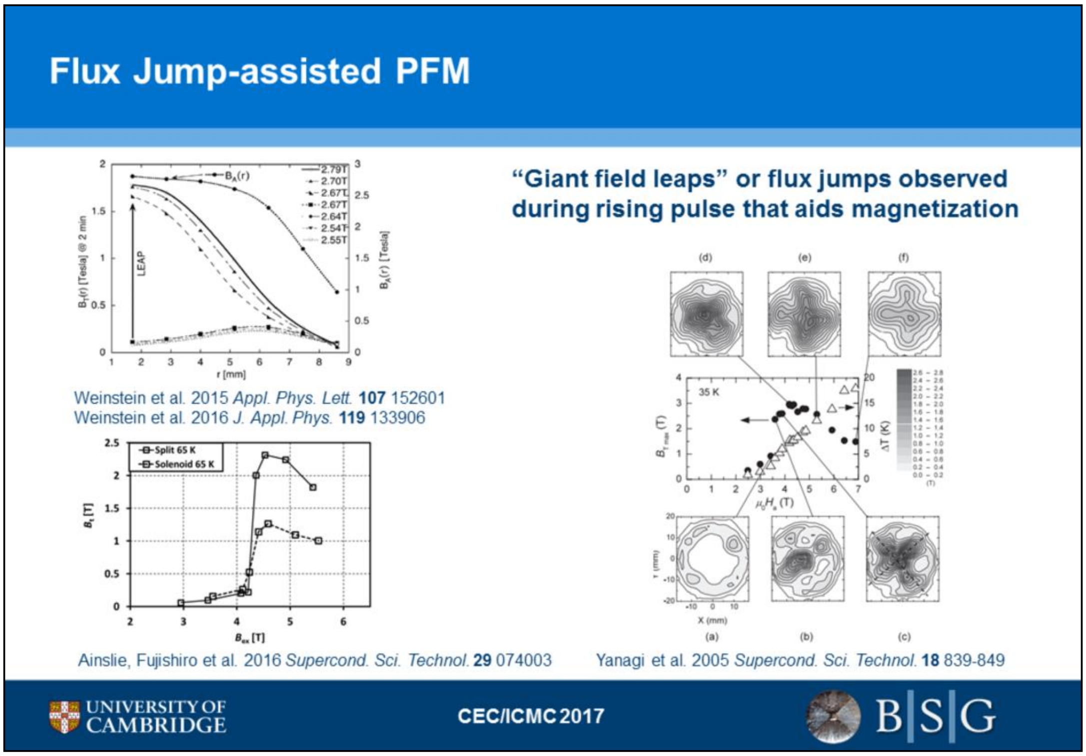

So-called 'giant field leaps' or flux jumps have been observed by a number of research groups investigating PFM, where a flux jump (or multiple flux jumps) occurs during the rise time of the applied pulsed field, resulting in a large increase in the measured trapped field at the centre of the top surface of the bulk sample and full magnetization. Although flux jumps can occur at any point during the magnetization process, exploiting flux jumps during the rise time of an applied pulse would enhance the trapped field in practical applications, as well as reduce the magnitude of the applied field required.

The figures show some examples of flux jump-assisted PFM in the literature from Yanagi et al., Weinstein et al., as well as our own research observations.

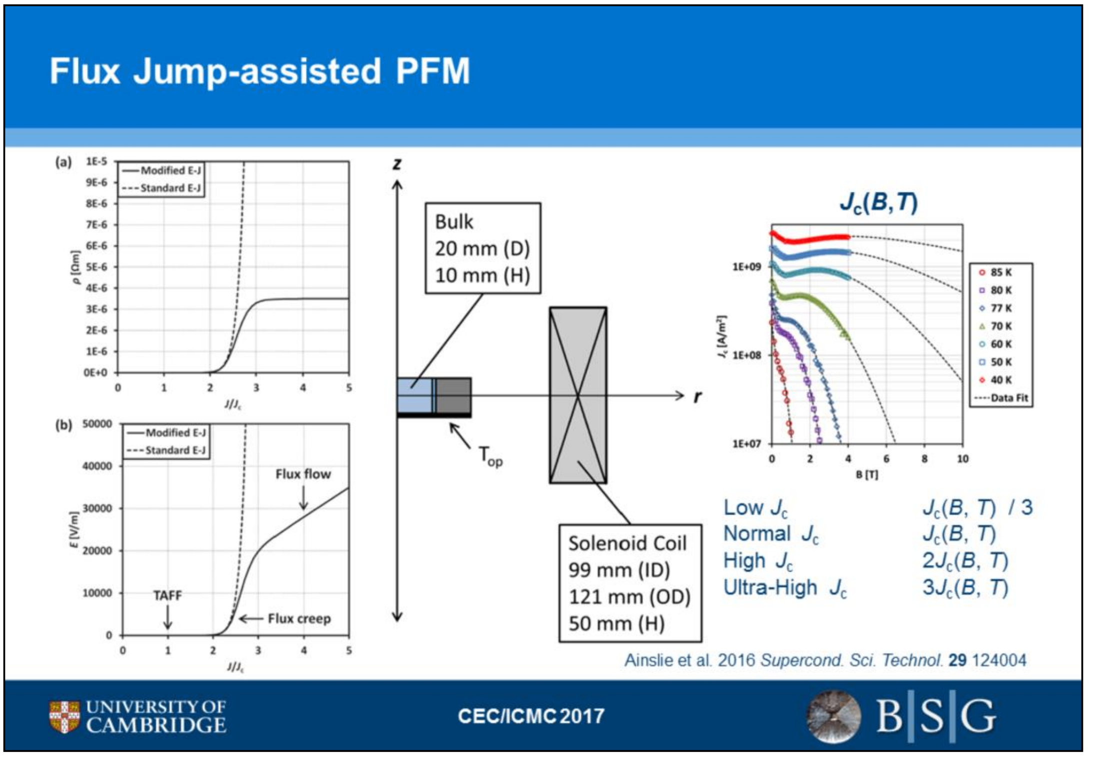

Another 2D axisymmetric model, similar to the previous split coil model, but using a solenoid coil magnetizing fixture (no iron yoke) was used to qualitatively reproduce the flux jump phenomenon to good effect. The same $J_c(B,T)$ characteristics (as presented earlier) were used as input data for the characteristics of the bulk superconductor, but low, high and ultra-high J_c samples were investigated by dividing or multiplying the $J_c(B,T)$ by an integer. This varies the magnitude of J_c, but maintains the overall pinning characteristics. A modified E-J power law characteristic representing the normal state resistivity when $J > J_c$ is implemented, which more accurately represents the different regimes of the E-J curve and improves the convergence properties of the numerical model.

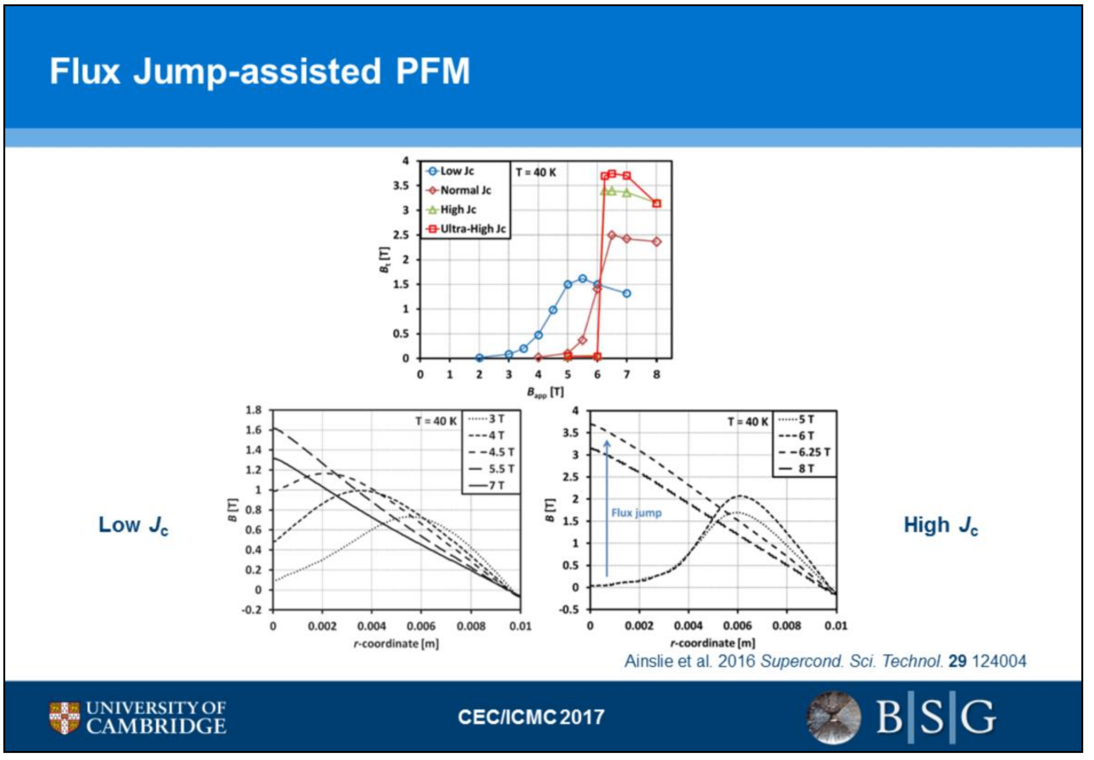

The top figure shows a comparison of the trapped field at the centre of the top surface of the bulk samples (r = 0mm) at a height of z = +0.1 mm at t = 300 ms (pulse rise time = 15 ms) for applied fields up to 8 T and at an operating temperature of 40K. For the high J_c and ultra-high J_c samples, there is a large increase in the trapped field for a relatively small increase in applied field (+0.25 T) above 6 T, which is qualitatively consistent with the observed experimental results. For increasing applied field values after the sample is fully magnetised, the trapped field begins to reduce due to an increasing temperature rise generated by the more rapid movement of flux lines in the sample. The bottom two figures show the trapped field profile across the top surface for the low Jc (left) and high Jc (right) cases. No flux jumps are observed on the left and the magnetic field steadily penetrates the sample with increasing field. On the right, however, the trapped field profile suddenly changes between an applied field of 6 and 6.25 T, again qualitatively consistent with experimental results.

Towards ultra-light rotating machines for next-generation transport & power applications

UNIVERSITY OF CAMBRIDGE

CEC/ICMC 2017

B|S|G

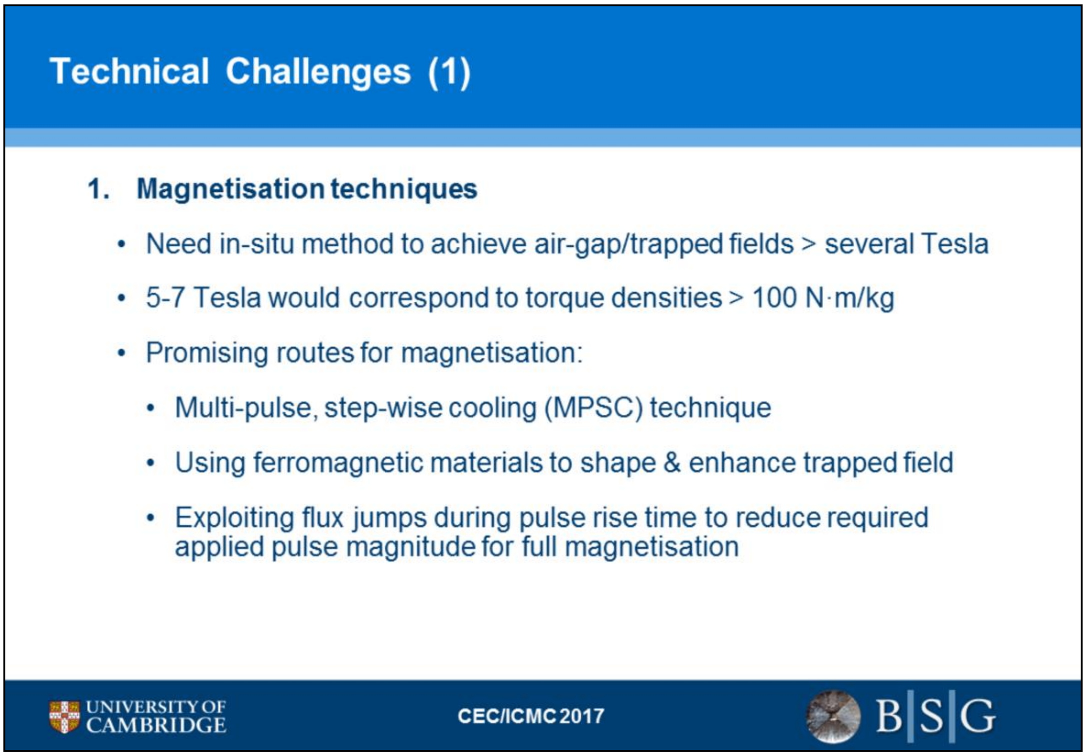

In June 2016, the Bulk Superconductivity Group organized a roadmapping workship in Cambridge to identify where the field may develop over the medium and long terms and to align the research strategy of the academic community to the needs and requirements of its industrial partners. One of the applications under the spotlight was ultra-light superconducting motors and generators, and the following slides summarise the major technical challenges that must be overcome to enable the development of improved demonstrators and application-specific prototypes for real world applications.

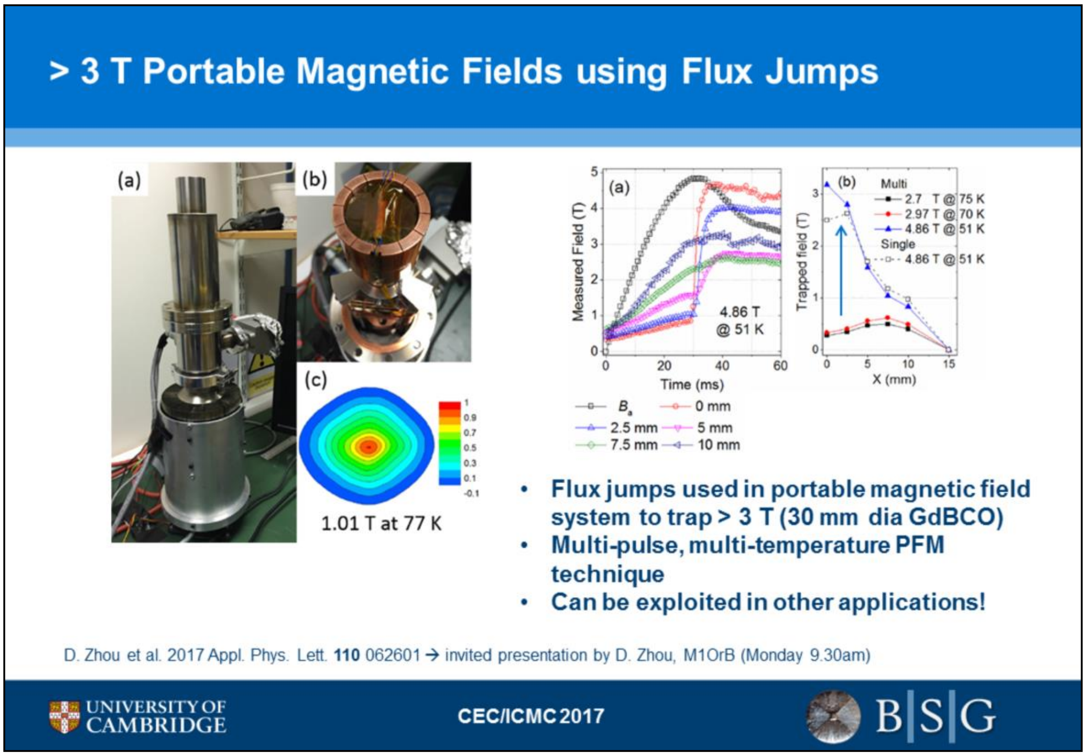

Such flux jumps were recently exploited in a portable magnetic field system to trap a surface magnetic field of > 3 T in a 30 mm diameter Gd-Ba-Cu-O sample. The magnet system operates between 50-60 K using a portable Stirling cryocooler (Cryotel CT, Sunpower) and flux jump behavior was consistently observed when the applied field exceeded a critical value (e.g., 3.78 T at 60 K). A multi-pulse, multi-temperature PFM technique, where the bulk is ‘pre-charged,’ or partially magnetized, with magnetic flux approximately half way to the middle of the sample at higher temperatures of 75 K and then 70 K, is then used to facilitate a flux jump that fully magnetized the sample > 3 T at 51 K (applied field of 4.86 T). This technique can be exploited in other applications, including superconducting machines.

Technical Challenges (2)

2. Magnetic field stability

- Real machine environment can lead to demagnetisation of bulks (possibly full demagnetisation)
  - Bulks can be exposed to time-varying magnetic field fluctuations

  → AC losses, shielding current redistribution
  - Logarithmic flux creep
- Understanding & predicting response of magnetised bulks in complex machine environment is crucial

→ Long-term machine testing, mitigation methods to supress trapped field attenuation (including shielding), strategies for re-magnetisation

Technical Challenges (3)

3. **Mechanical properties (bulks & machine)**
   - Mechanical properties of bulks are limiting factor for high field applications
     - Internal reinforcement by tuning material processing & constituent materials
     - External reinforcement using high-strength metal (or metal alloy) rings or other techniques
   - For machine design, careful analysis of mechanical design required due to increased electromagnetic forces

UNIVERSITY OF CAMBRIDGE CEC/ICMC 2017 B|S|G

Technical Challenges (4)

4. Numerical modelling

- Analytical & numerical models continue to improve & increase in complexity
- Further development is needed in the following areas:
  - Application-specific performance evaluation of bulks under specific magnetising & operating conditions
  - Multi-scale electric machine modelling to assess electromagnetic & mechanical performance
    - Such models should easily represent both conventional & superconducting materials, as well as moving/rotating parts

UNIVERSITY OF CAMBRIDGE — CEC/ICMC 2017 — B|S|G

Key Enabling Applications

- Replacing permanent magnets with bulks could have very high power densities
- However, cost is also likely to be high & the design complex
  - Best applications to benefit are where size & weight is a significant cost driver:
    - POWER GENERATION in next-generation wind power generators
    - FUTURE TRANSPORT in electric aviation & ship propulsion
      - NASA & Airbus have suggested power densities > 25 kW/kg are required → superconducting machines
- For more information & summary of the recent UK Bulk Superconductivity Roadmapping Exercise, please visit:

  https://www.repository.cam.ac.uk/handle/1810/256650

UNIVERSITY OF CAMBRIDGE | CEC/ICMC 2017 | BSG

Key Enabling Applications

- Replacing permanent magnets with bulks could have very high power densities
- However, cost is also likely to be high & the design complex
  - Best applications to benefit are where size & weight is a significant cost driver:
    - POWER GENERATION in next-generation wind power generators
    - FUTURE TRANSPORT in electric aviation & ship propulsion
      - NASA & Airbus have suggested power densities > 25 kW/kg are required → superconducting machines
- For more information & summary of the recent UK Bulk Superconductivity Roadmapping Exercise, please visit:

  https://www.repository.cam.ac.uk/handle/1810/256650

UNIVERSITY OF CAMBRIDGE

B|S|G

Acknowledgements

The authors are grateful to
Dr. Yoshitaka Ito
(IMRA Material R&D Co., Ltd.),
and Prof. Philippe Vanderbemden
(University of Liège)
for providing slides.

UNIVERSITY OF CAMBRIDGE

National University Corporation
TUMSAT
Tokyo University of Marine Science And Techology